Problem 1 - Galton board

International Physicists' Tournament-Greek Team[1]

[1] *National and Kapodistrian University of Athens, Physics Department.*

HELLENIC REPUBLIC
National and Kapodistrian University of Athens
EST. 1837

INTERNATIONAL PHYSICISTS' TOURNAMENT

Contents

1 Introduction **1**

2 Theoretical Model **1**
2.1 Mathematical Formalism . . . 1
2.2 Motion inside the lattice . . . 2
2.2.1 Lattice interactions . . . 2
2.2.2 Vertical motion . . . 2
2.3 The stochastic process . . . 2
2.4 Central Limit Theorem (CLT) . . . 3

3 Methods **3**
3.1 **1st** experimental procedure . . . 3
3.2 **2nd** experimental procedure . . . 3
3.3 Computational methods . . . 4

4 Analysis **4**
4.1 Steady board . . . 4
4.2 Vibrating Board . . . 5

5 Discussion **5**
5.1 Conclusions . . . 5
5.2 Future work . . . 5
5.2.1 Further experiments and simulations . . . 5
5.2.2 A machine learning approach . . . 5

Problem 1 : Galton Board

Abstract

The Galton board is a simple yet effective device that demonstrates how the Central Limit Theorem applies to a physical system and allows for the visualization of discrete probability distributions, such as the binomial distribution, which approximates the normal distribution. This work investigates the physical parameters of the board that determine the final distribution of the beads, aiming to generate non-normal distributions. We focus on the features of the distributions in order to examine if the Central Limit Theorem applies when certain conditions are met. We further explore the effects of a vibrating board. In order to study the motion of the objects on the board, an original, problem-specific notation has been developed based on the random walk stochastic process. Two different experimental setups were constructed to perform tests with changing variables and a vibrating motion which were compared to numerical simulation results. The experimental and theoretical results as well as future study prospects are discussed.

1 Introduction

The Galton board can depict the way a normal distribution emerges naturally in chaotic phenomena. Beads are dropped from above and, after colliding with pegs placed on the board, fall into bins at the bottom end of the board. The distribution of the beads in the bins can be viewed as the discrete probability density function (PDF) of the final positions of the beads. Furthermore, the heights of the beads' columns in the bins create the histogram of the distribution. In the original version of the board, the distribution of the beads in the bins is a binomial distribution. Given a large enough number of beads, this binomial distribution approximates a normal distribution.

By modifying the physical parameters of the system, i.e. the size of the beads relative to the pegs, the peg shape and orientation, their positioning on the board, and the method in which the beads are dropped, one can obtain a number of different distributions of beads in the bins, some of which do not satisfy the Central Limit Theorem (CLT).

In this work, we explore the role of the aforementioned parameters in shaping the final distribution of the beads in the board's bins. In Sec. 2 we propose a stochastic theoretical model for the motion of the beads inside the lattice of pegs on the board. In Sec. 3 we detail our experimental process and setups and describe the numerical simulations we performed. Finally, we analyse and compare the results obtained through our three different methods in Sec. 4 and discuss the conclusions and future prospects of this work in Sec. 5.

2 Theoretical Model

2.1 Mathematical Formalism

The Galton board, from a stochastic process perspective, can be described as a two-dimensional lattice that consists of unit square cells (sc) of identical sizes [1]. The obstacles, such as pegs, interact with falling bodies. Each peg is located at the center of the cell and has characteristic dimensions and arrangement relative to the size of both the moving beads and the sc themselves. These characteristics dictate the physics of the interactions that will be further elaborated. When a bead falls and bounces on the obstacles centered in each cell of the board, it can be considered as a randomly navigating walker within this lattice. The bead, after interacting several times with the steady pegs, falls into one of the bins at the bottom of the board. To provide a more precise mathematical description of this scenario, we employ variables that aid in defining the dynamics of the system and are represented visually, as depicted in Fig. 1.

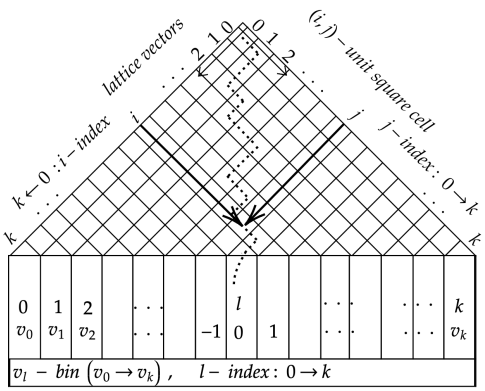

Figure 1: Notation of the 2D-square obstacle-centered lattice.

Certain assumptions must be made in order to analytically examine the stochastic process. First of all, it is assumed that the beads do not interact, which can be achieved by releasing each ball individually. Secondly, it is assumed that the downward velocity of the beads remains constant and that they follow a linear trajectory as they move from one cell to the next. Finally, speeds are assumed to be relatively small so that the beads cannot bounce back to a previous level. These assumptions correspond to a Galton board placed on an incline and a dense lattice of pegs.

The random walk of an individual bead within the lattice is notated according to the following formula.

$$(i,j) \longrightarrow \begin{cases} (i+1,j)\ ,\ with\ \ probability,\ P_{ij} \\ (i,j+1)\ ,\ with\ \ probability,\ 1-P_{ij} \end{cases} \tag{1}$$

Here (i,j) denotes the square cell that the bead is. The $P_{i,j}$ is the probability of the bead to fall to the left side of the object.

This model provides a broader framework for describing the motion and should not be seen strictly as a grid. For a different grid, the cells can dense, for missing obstacles new assumption can be taken such as $(i,j) \to (i+1, j+1)$, with $P_{i,j} = 1$ and so on. With this formalism, almost any possible grid can be manufactured.

The partition of a PDF will result to a vector with elements v_l (Right part of Fig. 4). Those can be described as $v_k = \frac{i-j}{2}$ or $v_k \in \left(\left\lfloor -\frac{i}{2} \right\rfloor, ..., \left\lceil \frac{i}{2} \right\rceil\right)$ if k is even or odd respectively.

Since in every cell the probability is independent, a path (from the start to the bottom of the board) has a probability equal to the product of the cells it contains. The probability $P_l(v_l)$ of the $l-$bin is the summation of all the $\binom{k}{l}$- paths that lead to l after $k+1$ steps.

$$P_l(v_l) = \sum_{v_{l-paths}=1}^{\binom{k}{l}} \prod_{i,j=0}^{i+j=k-1} P_{i,j} \tag{2}$$

Deriving the PDF using this method is a time-consuming process. A method using Markov Chain-alike tools will be used for this purpose [2].

2.2 Motion inside the lattice

2.2.1 Lattice interactions

The motion of the bead will be described as a two dimensional movement, where in the horizontal axis the bead performs a random walk and on the vertical axis falls similar to a body inside a media with drag.

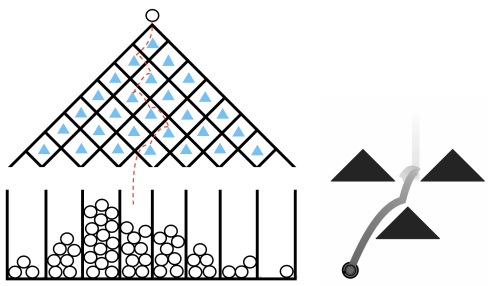

Figure 2: Left: Random walk of falling bead within the 2D-lattice. Right: Bead - obstacle impact for the angle model is tested computationally using a physics sandbox. The error was calculated for a big amount of repetition to be below 10^{-2}, accurate enough for the precision of the model.

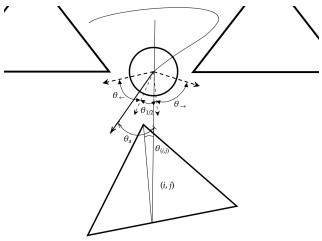

Figure 3: Angles in the bead - obstacle interaction.

After few interactions with the sides of the obstacles, the bead follows a final trajectory which as a first approximation has one degree of freedom, the angle θ_a-, a random variable following a Gaussian distribution with $\mu = 0$ and $3\sigma = 0.5\pi$ $Pr(\theta_a) = \frac{1}{\sigma\sqrt{2\pi}} e^{-\frac{1}{2}\left(\frac{\theta_a}{\sigma}\right)^2}$. If the obstacle is centered, due to symmetry the trajectory will be equally probable. In the case we change the obstacles angle $\theta_{(i,j)}$ then that probability changes too. In any case there will be an angle-range around the tip of the triangle for which the all angles can equally send the bead to both sides. The sharing angle is denoted as $\theta_{1/2}$, the angles that lead to left and right are denoted as $\theta_{\leftarrow}$ and $\theta_{\rightarrow}$ respectively . The probability of each sc is now given as:

$$P_{i,j} = \frac{\theta_{\leftarrow} + \theta_{1/2} \cdot 1/2}{\theta_{\leftarrow} + \theta_{1/2} + \theta_{\rightarrow}} \tag{3}$$

By changing $\theta_{(i,j)}$, $P_{i,j}$ can take a preferable value in the range that $\theta_{1/2}$ allows.

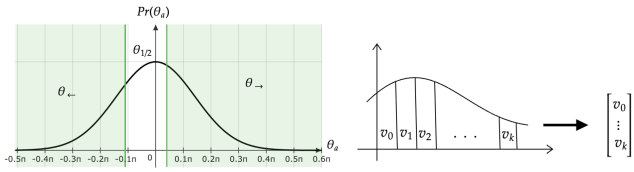

Figure 4: Left: PDF of the angle determining the trajectory. In the case of a twisted centered obstacle in a sc. Right: Distribution divided into areas and transformed into a vector.

Hence $P_{i,j} = P_{i,j}(\theta_{(i,j)})$. Transforming the probability matrix $[P_{i,j}] \longrightarrow [\theta_{i,j}]$ to an angle matrix.

$$\begin{bmatrix} (0,0) & (0,1) & \dots & (0,k) \\ (1,0) & & & \\ \dots & & \iddots & \\ (k,0) & \iddots & & 0 \end{bmatrix} \longrightarrow \begin{bmatrix} \theta_{0,0} & \theta_{0,1} & \dots & \theta_{0,k} \\ \theta_{1,0} & & & \\ \dots & & \iddots & \\ \theta_{k,0} & \iddots & & 0 \end{bmatrix} \tag{4}$$

The current method for producing the probability matrix is a bottom-up process, where the partition of the function translates to a number for each bin 4, then this number gets divided and passes to the above cells, where it gets normalized again and so forth. However, this process can be time consuming and counterproductive. Since several partitions can be made for each sc, it is important to find a way to optimize the process, so that the final probability matrix closely adheres to the theoretical model.

2.2.2 Vertical motion

It is assumed and confirmed experimentally using a pixel-video tracker that the velocity of a falling bead is similar to terminal velocity of falling through a non-dense medium $v_t \sim \sqrt{\frac{2mgsin\phi}{\rho \cdot A}}$, where m, A (mass,area) are characteristics of the bead, ϕ the angle of the board and ρ is proportional to the amount of cells/board area. Thus it's constant and a discrete time unit t_d can be defined. If seen as a diffusion process, a movement in the grid is the steps that are taken for every discrete time unit and is approximately equal to the mean free path $\sim \sqrt{t_d}$ and perpendicular to the fraction of the obstacle and cell size.

Until now the lattice motion has been examined, in the case of one step-random walk. The board's vibration can affect the mean free path and the step can possibly increase allowing movement between non-adjacent cells Eq.1, from one cell (i,j) to cell $(i+n, j+m)$, for $(n,m) \in \mathbb{N}^2$. This can affect the final distribution.

2.3 The stochastic process

The $k \times k$ board has $N = \frac{(k+1)(k+2)}{2}$ cells. By naming each sc from left to right in each row, a matrix can be formed, alike a Markov matrix.

P	1	2	3	4	5	...	N
1	0	$p_{(0,0)}$	$1-p_{(0,0)}$	0	0	0	0
2	0	0	0	$p_{(1,0)}$	$1-p_{(1,0)}$	0	0
3	0	0	0	0	$p_{(0,1)}$	...	0
4	0	0	0	0	0	...	0
5	0	0	0	0	0	...	0
...	...	...	...	...	...	...	...
N	0	0	0	0	0	0	0

This is the (right-)transition matrix $\mathbf{P}$ of the process and the elements are the transition probabilities with each row summing to 1. This process can be described by a sequence of possible events in which the probability of each event depends only on the state attained in the previous event.

Starting with a state given as a stochastic vector $\mathbf{v}^0 = [1, 0, ..., 0|0, ..., 0]$, whose elements are non-negative real numbers which sum to 1, the right vector side denotes the final state (the $k-$bins with v_l- elements), while the left side has $(k^2 + k + 2)/2-$ elements. The chain moves to consequent states at discrete time steps and after a finite sequence of k-transitions, where every change of state of the system is called a transition, the vector $\mathbf{v}^k = [0, ..., 0|f_0, ..., f_k]$ corresponds to the final state of the system, where $\sum_{l=0}^{k} f_l = 1$ and expresses the regular partition of the Probability density function.

$$\mathbf{v}^0 \cdot \mathbf{P} = \mathbf{v}^1 \rightarrow \mathbf{v}^1 \cdot \mathbf{P} = \mathbf{v}^2 \rightarrow ... = \mathbf{v}^k \tag{5}$$

In this way it is possible to examine which distribution a specific setup produces. A numerical program using Markov Chains has been used to evaluate the distributions for a given angle matrix. The reverse process can lead to finding the setup that produces a given distribution.

2.4 Central Limit Theorem (CLT)

Assuming that the distribution of the beads is characterized by a random variable following the distribution $f^{(0)}(s)$, where s represents the length along the i-th row and that each row of obstacles has a distinct distribution $g_i(s)$, the cumulative effect after numerous rows tends to approximate a normal distribution, particularly if the distributions $g_i(s)$ are consistent across all rows. This gradual process of curve smoothing through repeated convolutions can be described as the convergence towards a normal distribution.

$$f(s) \approx (...(f^{(0)} * g)*)g)*...)*g(s) = (...(f^{(1)} * g)*...)*g(s) \tag{6}$$

By adding a perturbation term to every i-row or if $g_i(s)$ changes per row as $f^{(0)} * (g + \delta g)(s)$, the final $f(s)$ will have additional corrections that can affect the distribution and differentiating it from the Binomial.

For the CLT [1] to apply to a PDF, a finite variance is required. However, numerous heavy-tail PDFs with infinite moments exist, such as the Cauchy and Lévy distributions. A more flexible alternative, the Generalized Central Limit Theorem (GCLT) [1], comes into play when the finite variance assumption doesn't hold. GCLT states that if sums of independent and identically distributed random variables (i.i.d.) converge to a distribution $X_i \xrightarrow{d} \mathscr{F}$, then $\mathscr{F}$ must be a stable distribution. Stable distributions possess the property that linear combinations of them (with positive coefficients) also result in a stable distribution. This class comprises four parametric distributions that lack a general analytical expression, including well-known PDFs like Cauchy, Lévy, Gaussian, and their various combinations.

For instance, a fat-tail distribution, like the Landau PDF, does not satisfy the conditions for the CLT, as it has infinite moments, but, as a stable distribution, it does satisfy the GCLT. Given that a Galton board can only accommodate a finite number of bins, if there is convergence after repeated experiments, the resulting distribution is expected to possess a mean and variance. Even if the sample approaches a heavy-tail PDF with non-finite moments, the theorem can still be applied in its generalized form.

3 Methods

3.1 1st experimental procedure

For the first setup, a desktop Galton board was constructed. Since the first experiment aimed at examining several parameters relevant to the positioning of the pegs and the properties of the beads, it was necessary for the peg distribution to be changeable. The construction had an opening in the back so that different wooden plates with pegs could be installed. Also, it featured three openings on its top end, one in the middle and two at the ends to allow for filling and emptying. Millimeter grid paper was installed in the background of the bins, so that the height of each distribution could be measured. A variety of sizes for the beads and pegs, as well as different configurations for the positions of the pegs were used. The initial height from which the beads were dropped could be adjusted as well, by use of a small pipe [experiment 1 video].

Figure 5: **1st** experimental setup.

3.2 2nd experimental procedure

A second setup was devised in order to control the orientation angles of each obstacle. This Galton board was constructed of lightweight cardboard in particular with thin wood sheet. The obstacles were made from the same materials, while a light plexiglas sheet covered the setup so that the beads would not slip away [experiment 2 video].

This experimental layout facilitated the introduction of vibration. Two one-meter-long lubricated axes functioned as the driving mechanism for four roller bearings, supporting the board in an incline form of 45° degrees. There were two beams connected to the same side of the board also linked to two rotational metal DC geared motors. These motors were responsible for converting rotational motion into oscillatory movement, allowing for the controlled vibration of the board. By

increasing the frequency of the oscillations, the desired vibration was achieved. The motors operated at approximately 110 rotations per minute (rpm). Precise adjustment of the velocity was possible through a small transformer linked to the power source, which maintained voltage and torque, preventing any displacement of the board. Balls of 6*mm* were used.

Figure 6: 2nd experimental setup.

3.3 Computational methods

We developed a code based on pymunk (2d rigid body physics library used in Python)[4] so as to obtain distributions other than the normal distribution.

The simulations conducted incorporate various modifications to the classic Galton board setup. These modifications include using circular pegs and beads achieving the binomial-normal distribution, employing square-shaped pegs to approach the uniform distribution, utilizing triangles with specific corner analogies to obtain the lognormal distribution, altering the angles of isosceles triangles in order to study the shifting of distributions, exploring the resemblance of normal distributions using equilateral triangular pegs, experimenting with the separation of a single distribution into two using a large 45° isosceles triangular obstacle in combination with circular pegs and utilizing square-shaped beads along with circular pegs. Snapshots of four of the simulations we performed can be seen in Fig. 7 and in the [simulation-video].

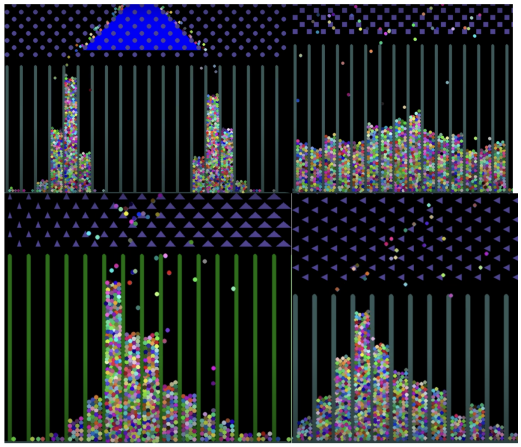

Figure 7: Simulations.

We also explored the problem via employing Markov chain Monte Carlo codes [2]. We developed our code routines by adding in every matrix element a small fluctuation. Also a monte carlo simulation for a horizontally oscillating falling object in a grid has been developed to further comprehend the effects of vibration.

4 Analysis

The experiments and simulations provided data, summarized in Table 1, for a variety of angle distributions. For each distribution an average sample was kept. Also, histograms Fig. 9, Fig. 10 and Fig. 11 were chosen for the visualization of the samples retrieved from the experiments, Monte Carlo simulations and the pymunk rigid-body simulations. The expected PDF is represented by a scatter plot with solid lines.

4.1 Steady board

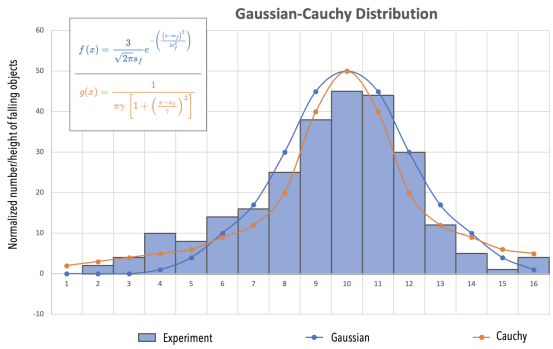

Figure 8: Gaussian - Cauchy distribution comparison.

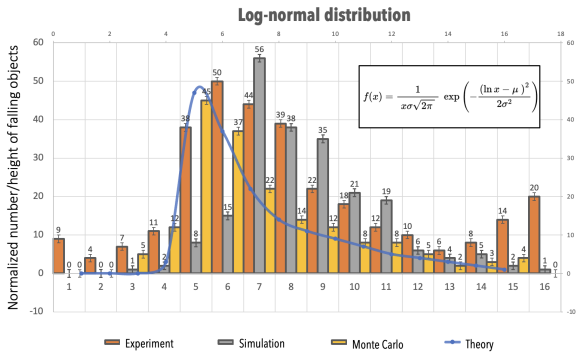

Figure 9: Log - Normal distribution.

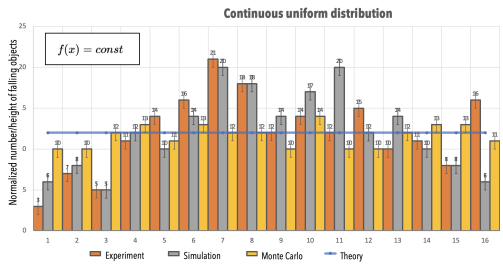

Figure 10: Continuous uniform distribution

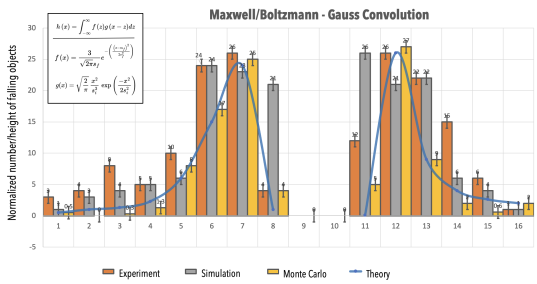

Figure 11: Maxwell/Boltzmann - Gauss convolved distribution.

In order to draw conclusions regarding the data of each distribution produced through different methods, the resulting

samples were compared. To confirm that two histograms are statistically equivalent, we used the Kolmogorov-Smirnov (KS) test. This test checks the hypothesis that two samples come from the same specific distribution. If the p-value is high, there are no statistically significant differences. For the extreme values of the data the Anderson-Darling test is used instead, which assigns greater weight to the tails of the distribution. This test provides more sensitivity compared to the KS test.

Statistical equality / KS-test			
PDF	Experiment	MCMC	Simulation
Gauss	0.530	0.747	0.642
Cauchy	0.821	0.328	0.661
LogNorm	0.354	0.819	0.772
Uniform	0.092	0.128	0.320
Maxwell	0.595	0.212	0.046
Rand PDF1	0.094	0.734	0.181
Rand PDF2	0.039	0.595	0.455

Table 1: p values between the fitted PDFs and the samples obtained by each method. The significance level of p value is set at 0.05, hence the calculated index in the most cases is lower and can confirm that is unlikely to have occurred by random chance.

4.2 Vibrating Board

The observed results were similar to the expected for lower rpms or shorter movement higher rpm vibration. Since they are categorical variables, χ^2 is used.

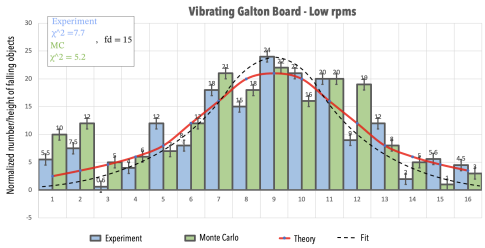

Figure 12: Distribution at vibrating board at low rpm

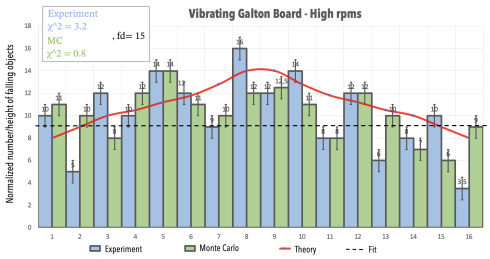

Figure 13: Distribution at vibrating board at high rpm

Overall, the effects of the low-rpm oscillations and the vibration (short and fast motion) where limited in most cases in changing characteristic parameters of the theoretically expected PDFs. The higher-rpm oscillation in many cases flattened the expected curve. This was expected since this interaction increases the number of possible steps per movement, allowing the beads in the same falling time to strew further from the expected one step per discrete time unit walk.

While the system oscillates, shocks might occur that affect the motion of the beads. Those are minimized with lower rpms. In the steady board the beads falls separately, since the random walk motion does not take into consideration bead-bead interactions. In the second case, as showed in the experiment's video, this is not required. Though as explained, those interactions don't affect the $Pr(\theta_a)$ PDF, but it is likely the σ, μ parameters.

5 Discussion

5.1 Conclusions

The first setup, Fig. 5, tested several parameters such as different falling objects, peg distributions. Those changes didn't seem to affect the final PDF.

The second setup, Fig. 6, focused on the obstacles and the results of this experiment seem to be in agreement with the various methods and the theoretically expected distributions. It is important to note that even though the lattice model based on the angles has strict restrictions for the motion of each bead, the deviations that occur statistically will nullify each other.

It can be stated that a PDF can or cannot satisfy CLT or GCLT. But in practice in an i.i.d. scenario where the sum of those variables converges to a distribution, this will satisfy some form of the CLT, but it will not necessarily produce a light tail distribution. A skewed and fat tailed distribution does not satisfy the CLT but the convergence will satisfy the GCLT. This is because those distributions may lack finite variance, but they still exhibit a form of stable behavior when combined.

The bimodal distributions that were created, emphasize the divergence from the Gaussian distributions. In many cases the Boltzmann distribution characteristics were expected since this setup had obstacle-angles that kept the trajectories almost the same for the falling objects, hence the movement was determined by the velocities similar to the ideal gas model. The Log-Normal distribution is expected for variables following $Y = X_1 \cdot X_2 \cdot \ldots \cdot X_k$ and this can be proved by taking the $logY$ and applying the CLT. The Cauchy and Gaussian distributions, as well as many skew distributions were difficult to be compared. These distributions stochastically can be mixtures of each other, hence the model cannot easily distinguish them.

5.2 Future work

5.2.1 Further experiments and simulations

A vertical vibration will be examined experimentally as well with a similar setup. Currently the simulation is being further developed to add an oscillatory motion to the beads. More experiments and simulations will be done, focusing on the combination and different parameters to approach other possible corrections to the theory.

5.2.2 A machine learning approach

To address the challenges of producing a probability matrix, a Machine Learning algorithm is being developed. This requires a data base with matrices produced using the Markov matrix and the final-state vectors and will be able to produce several probability matrices that result to the same vector, perform MCMC simulations for each and determine the probability which reproduces the assumed PDF most accurately and also satisfies Eq. 3.

References

[1] A. Papoulis and S. Unnikrishna Pillai, 2002, Probability, Random Variables and Stochastic Processes, McGraw-Hill Europe

[2] S. Brooks, A. Gelman, G. L. Jones, X-L. Meng, 2011, Handbook of Markov Chain Monte Carlo, Chapman and Hall/CRC

[3] S. Petrov, Python Galton Board, 2020

[4] V. Blomqvist, Pymunk, 2007-2023